Electrochimica Acta 56 (2011) 5214–5221

Contents lists available at ScienceDirect

Electrochimica Acta

journal homepage: www.elsevier.com/locate/electacta

Modulation of the interfacial electrochemistry of surfactant-functionalised polypyrrole chemical sensor systems

Faiza J. Iftikhar, Priscilla G.L. Baker*, Abdul M. Baleg, Peter M. Ndangili, Stephen N. Mailu, Emmanuel I. Iwuoha

Sensorlab, Department of Chemistry, University of the Western Cape, Private Bag X17, Bellville 7535, South Africa

ARTICLE INFO

Article history:
Received 27 October 2010
Received in revised form 10 March 2011
Accepted 10 March 2011
Available online 17 March 2011

Keywords:
Polypyrrole
Surfactants
Diffusion coefficients
Electrochemical impedance spectroscopy
Cyclic voltammetry

ABSTRACT

The redox properties of electro-polymerized polypyrrole (Ppy) doped with different surfactants were studied in acid medium. It was found out that the addition of different surfactants affect the redox properties as evidenced by diffusion coefficients and rate constants calculated from experimental data obtained from cyclic voltammetry (CV) and electrochemical impedance spectroscopy (EIS). Three different surfactants were incorporated into polypyrrole matrix to form homogeneous composites i.e. anionic surfactant polyvinylsulphonic acid (PVSA) as well as non-ionic surfactants (polyethylene glycol p-(1,1,3,3-tetramethylbutyl)-phenyl ether (Triton-X 100) and polyoxyethylene (20) sorbitan monolaurate (Tween 20). CV and EIS experiments were carried in the presence of the redox probe $K_3[Fe(CN)_6]$. Diffusion coefficient was interpreted as a measure of electron movement within the composite polymer structure and rate constant was interpreted as a measure of the rate of oxidation and reduction of the redox probe. The highest value for diffusion coefficient and rate constant was obtained for Ppy/PVSA as 8.16×10^{-12} cm^2 s^{-1} and 1.05×10^{-5} cm s^{-1} respectively. The values obtained by CV and EIS were in good agreement.

1. Introduction

Among the conjugated conducting polymers, polypyrrole Ppy is one of the most promising for technological and biomedical applications because of its aqueous solubility, its stability under environmental conditions, thermal stability, biocompatibility and biodegradation and therefore find wide applications [1–5]. The incorporation of a surfactant into a conducting polymer is likely to improve the electrical, theromooxidative, and hydrolytic stability due to the introduction of bulky hydrophobic component.

Poly(3-methoxythiophene) (PMOT) was electropolymerized in aqueous micellar media using different (anionic, cationic, neutral) surfactants and spectroscopic and electrochemical properties were investigated to study the influence of different types of surfactants on PMOT at the Pt electrode by Fall et al. [6] and it was shown that faradic yield notably increased from cationic to anionic surfactants. Polypyrrole has also been synthesized in the presence of the sodium salt of docecylsulphate (SDS) and docecyl-benzenesulphate (SDBS) and higher diffusion coefficients as compared to Ppy were reported [7]. In an important and related study by Li et al., where the mediating effect of surfactants on electron transfer was investigated, they concluded that the cationic tetradoceyltrimethylammoniumbromide system was better than the zwitterionic tetradoceyldimethylamine-oxide and anionic SDS in mediating electron transfer of fullerenes C60 on gassy carbon electrodes [8]. In a follow up study performed at glassy carbon electrodes coated with MWCNT/surfactant films in ionic liquid and phosphate buffer solution using cyclic voltammetry they concluded that surfactant hydrophilic groups play an important role in electrochemical behaviour of MWCNT [9].

In another research, conducting and stable polypyrrole (Ppy) was synthesized by chemical oxidative polymerization of pyrrole in aqueous solution containing an oxidant, ferric sulfate, and surfactants i.e. anionic, cationic and non-ionic surfactants including poly(ethylene oxide) (10), iso-octylphenyl ether (Triton X-100), poly(ethylene oxide) (20) sorbitan monolaurate (Tween 20) [10]. They observed that the mechanical properties and surface smoothness of Ppy films prepared from the aqueous solutions with addition of the non-ionic surfactants were greatly improved in comparison with those of Ppy prepared from the aqueous solutions in the absence of surfactants. The addition of surfactants accelerated the polymerization. It was also concluded that the interaction of cationic and non-ionic surfactants with Ppy under similar conditions was much weaker and such surfactants do not have any notable effect on the physical properties of polypyrrole.

Kudoh et al., described a chemically prepared Ppy having an enhanced conductivity and environmental stability under the coexistence of a sulphonic acid surfactant and a phenol derivative

* Corresponding author. Tel.: +27 219593051.
E-mail address: pbaker@uwc.ac.za (P.G.L. Baker).

0013-4686/$ – see front matter © 2011 Elsevier Ltd. All rights reserved.
doi:10.1016/j.electacta.2011.03.034

with an electron withdrawing group. The yield of Ppy depended on the concentration of the surfactant and conductivity of Ppy increased with increasing strength of electron withdrawing force of the substituent [11]. Shen et al., have also studied the effect of sulphonic acids on solubility, electrical and thermal properties of Ppy prepared by in situ doping polymerization [12]. Therefore the surfactants serve to improve the conductivity, stability and solubility in organic solvents and processibility. Sun and Ruckenstein have studied the effect of non-ionic surfactants on Ppy-bearing conductive composite by an inverted emulsion method and have discussed that HLB (hydrophilic lypophilic balance) with respect to non-ionic surfactants have an effect on the conductivity of the film formed [13].

Here we report on electrochemical synthesis and characterization of surfactant doped polypyrrole based on CV and EIS in order to provide a quantitative assessment of electron transfer processes at the interface of the polymer composite thin films. We have selected an anionic surfactant which is the sodium salt of polyvinylsulphonic acid (PVSA) for comparison to two neutral surfactants, Triton-X 100 (TX) and Tween 20 (TW) in order to investigate the effect on morphology and electrochemistry of surfactant modified polypyrrole. The surface morphology was studied to observe the effect of doping on surface area, since surface area may be related to efficiency of catalytic systems.

Literature indicated that cationic surfactants were less likely to affect physical properties of polypyrrole and thus no cationic surfactants were included for the study of interfacial electrochemistry of the surfactant modified polypyrrole thin films.

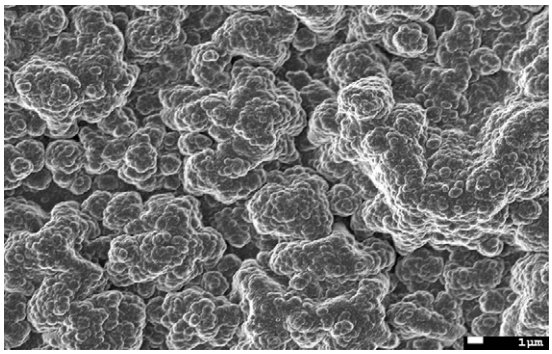

Fig. 1. SEM of undoped polypyrrole.

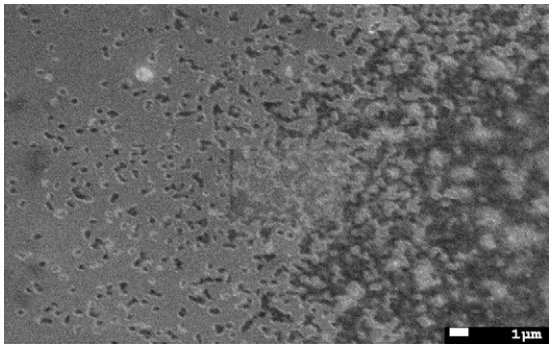

Fig. 2. SEM PPy/PVSA.

2. Experimental

2.1. Reagents and apparatus

Polypyrrole was doped with a ratio of 1:1, 1:0.6, 1:0.4 with respect to Triton-X 100 (TX), Tween 20 (TW) and sodium salt of polyvinylsulphonic acid (PVSA). Pyrrole as supplied by Sigma–Aldrich was distilled at reduced pressure, saturated with Argon gas and kept in dark at 4 °C. The surfactants used were Triton-X 100, Tween 20 and sodium salt of polyvinylsulphonic acid (PVSA) using 200 μl in each case and were supplied by Supelco, Sigma–Aldrich respectively and were used as provided. The electrolyte used in the polymerization and all electrochemical characterization experiments was prepared from hydrochloric acid (32%) and distilled water (specific resistance 18 MΩ, MilliQ, Millipore)

2.2. Methods

Scanning electron microscopy (SEM) was performed on JSM 7500F Scanning Electron Microscope, JEOL Ltd. The surfactant modified polypyrrole composites were prepared on screen printed gold (SPAu) electrodes by electrosynthesis and the electrodes were not coated for viewing. The Ppy composite film was grown in situ by cyclic voltammetry at 50 mV s^{-1} for 15 cycles in a solution containing the respective surfactant.

Cyclic voltammetric (CV) experiments were carried out using BAS 50 W integrated automated electrochemical workstation (Bioanalytical Systems, USA). A three electrode electrochemical cell was used with a platinum disk electrode (surface area of 0.0201 cm^2) as the working electrode (WE). The WE was cleaned with alumina slurries of 0.1, 0.3 and 0.05 μm fine alumina powders to a shiny finish. The working electrode was sonicated with ethanol and finally rinsed with distilled water for removing any impurities on the surface of the electrode. The reference electrode used was an Ag/AgCl electrode and the counter electrode was a polished fire treated platinum wire (1 mm × 5 cm). The monomer, 0.1 M pyrrole was polymerized in the presence of different dopants in 0.05 M HCl and the colour of the film was noted. Over-oxidation of the film was avoided in order to produce films with the highest possible conductivity. The concentration of the dopant in each case was calculated to provide a ratio of dopant to polymer as close to 1:1 as possible. The characterization of the polypyrrole films were carried out in 0.05 M HCl at different scan rates. 2, 4 and 6 mM $K_3[Fe(CN)_6]$ in 0.1 M HCl was used as redox probe for enhanced electrochemical signal during oxidation and reduction electron transfer at the interface of composite films in solution.

Electrochemical impedance spectroscopy measurements (EIS) on the thin films of polypyrrole composites were made using a PGZ402 Voltalab Analyzer (Radiometer Analytical, France) and the same three electrode cell arrangement and electrolyte as for CV. An AC amplitude of 10 mV and a frequency range of 50 KHz to 100 mHz with 20 steps per frequency decade was used and the potential was stepped between 100 and 500 mV at 100 mV intervals. The impedance data was modeled as equivalent electrical circuits using Z-view software.

3. Results and discussion

3.1. Scanning electron microscopy (SEM)

The SEM of undoped polypyrrole showed a uniform high surface with a high degree of roughness and corrugation with a strong resemblance to a head of cauliflower (Fig. 1).

SEM of composites formed by doping Ppy with surfactant show that the characteristic features of polypyrrole were replaced by distinctly different morphology in each case indicating the incorporation of the dopant into the polymer, to form a dispersion of the resulting composite at the electrode surface during electropolymerization. Ppy/PVSA formed a dense surface layer closely following the original cauliflower template of polypyrrole (Fig. 2).

It is proposed that the net positive charge on polypyrrole during oxidation facilitated the electrostatic incorporation of the anionic surfactant during each cycle of the polymerisation resulting in the observed dense patterning with much higher surface area. The Ppy/TW and Ppy/TX composites based on the incorporation of neutral surfactants, displayed an irregular distribution of phase separated islands of Ppy (Fig. 3a and b). This may be attributed to agglomeration in the presence of the surfactant during electrosynthesis, resulting in exclusion from the composite matrix.

3.2. Cyclic voltammetry

Ppy was electro-polymerized by cycling for 15 cycles from −400 to +700 mV at 50 mV s^{-1} in 0.05 M HCl with and without adding surfactants. The undoped polypyrrole was observed to have a yellow colour in the neutral state, which changed to intensely dark blue (almost black) as it was oxidized from −400 to +700 mV under inert atmosphere. Ppy/PVSA thin film was observed to have a blue colour whereas Ppy/TW was yellow in the oxidized state and the Ppy/TX film had a final dark yellow colour, after in situ electrosynthesis. The resulting composite films each were then characterized in acid medium in the presence of $K_3[Fe(CN)_6]$ and the oxidation and reduction peak currents were used to calculate the diffusion co-efficient using the Randles-Sevčik equation,

$$I_p = (2.69 \times 10^5) A n^{3/2} C_O D^{1/2} v^{1/2} \quad (1)$$

where I_p is the peak current, A is the geometric surface area of the electrode, n is the number of electrons transferred during the redox reaction, C_O is the concentration of the species oxidized or reduced, D is the diffusion coefficient and v is the scan rate. A plot of I_p against the square root of the scan rates, was used to obtain diffusion coefficient from the slope for anodic and cathodic processes. Furthermore the diffusion coefficient was incorporated into the Nicolson [14] equation given as

$$k_s = \frac{\Psi(\pi a D)^{1/2}}{\gamma^{\alpha}} \quad (2)$$

where, $\gamma = D_O/D_R$, and $a = nFv/RT$, F, R and T are the notations for Faraday constant, gas constant and temperature respectively. Using suitable textbook values for constants, a value for the rate constant k_s, was calculated. In this equation ψ depends upon peak to peak difference ΔE_p which can be obtained from the original paper of Nicolson [14] otherwise the values not found were calculated by the following empirical Eq. [15],

$$\Psi = (-0.6288 + 0.0021X)\,(1 - 0.017X) \quad (3)$$

where $X = \Delta Epxn$, expressed in mV.

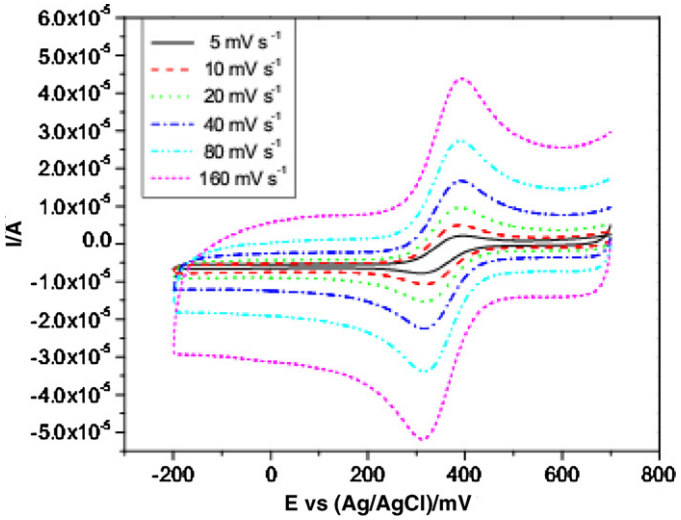

Fig. 4. Cyclic voltammetry of Ppy at Pt electrode in 6 mM $K_3[Fe(CN)_6]$ in 0.1 M HCl at different scan rates.

3.2.1. Pyrrole and polypyrrole composite films

The cyclic voltammograms for undoped polypyrrole thin film at different scan rates in a solution of $K_3[Fe(CN_6)]$ show one set of peaks and an increase in peak current associated with the oxidation and reduction of Fe^{3+}/Fe^{2+} with increasing scan rates (Fig. 4).

The graphs plotted for I_p vs the square root of scan rate confirm diffusion controlled kinetics for the system at all scan rates. The slope obtained for the cathodic process was 9.27×10^{-5} ($r = 0.997$) and the slope for the anodic process was 8.42×10^{-5} ($r = 0.993$). The ΔE_p value shows an increase with increase in scan rate at scan rates greater than 5 mV s^{-1} and the ratio of I_{p_a}/I_{p_c} was consistently observed to be close to unity, indicating near reversible electron transfer at the interface.

In a similar experiment using Ppy/PVSA, E_{pc} was shifted towards negative potentials with increasing scan rate, indicating some retardation of electron transfer within the bulk material of the composite film (Fig. 5). The ratio of I_{p_a}/I_{p_c} for Ppy/PVSA was 1.23 at 5 mV s^{-1} and decreased to 0.93 at 200 mV s^{-1}. The peak to peak difference ΔE_p was observed to increase with increasing scan rate, indicating the Ppy/PVSA thin film conformed to quasi reversible electron transfer kinetics at higher scan rates. The slopes obtained were 8.14×10^{-5} ($r = 0.999$) and 9.22×10^{-5} ($r = 0.997$) for anodic and cathodic processes respectively. The magnitude of the peak currents recorded were highest with Ppy/PVSA as compared to Ppy/TW and Ppy/TX or even undoped pyrrole itself, indicating that the most effective catalysis may be observed at the

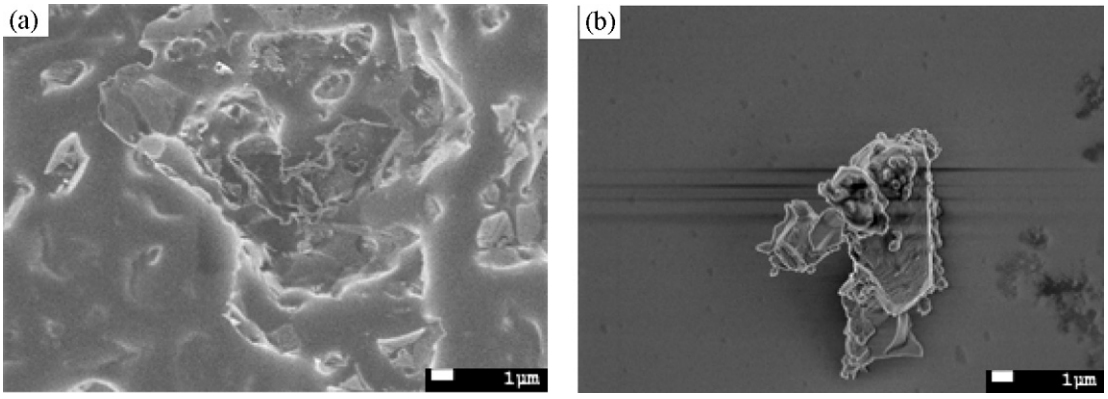

Fig. 3. (a) SEM of Ppy/TW and (b) Ppy/TX.

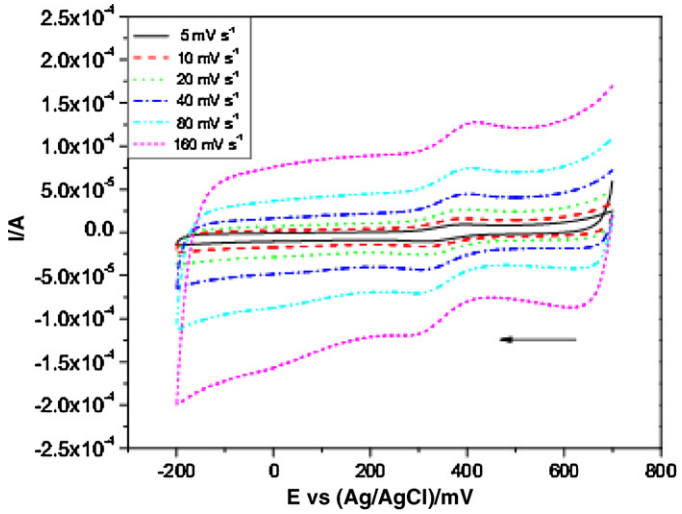

Fig. 5. Cyclic voltammetry of Ppy/PVSA at Pt electrode in 6 mM $K_3[Fe(CN)_6]$ in 0.1 M HCl at different scan rates.

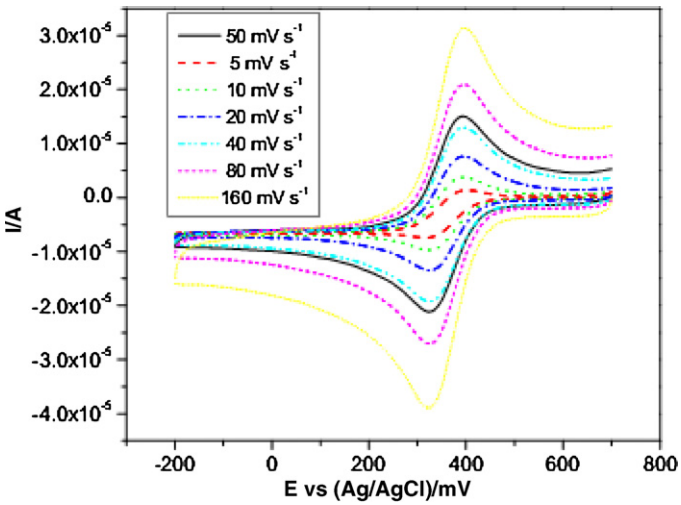

Fig. 7. Cyclic voltammetry of Ppy/TX at Pt electrode in 6 mM $K_3[Fe(CN)_6]$ in 0.1 M HCl at different scan rates.

Ppy/PVSA. Ppy/TW (Fig. 6) and Ppy/TX (Fig. 7) thin films similarly displayed quasi reversible electron transfer kinetics with comparable diffusion coefficients and regression analysis for oxidation and reduction of $K_3[Fe(CN)_6]$ at scan rates from 5 to 200 mV s^{-1}.

A comparison of the capacitive currents measured for the undoped and doped Ppy thin films, under the same experimental conditions, revealed a comparatively large baseline separation for the Ppy/PVSA system compared to undoped Ppy, Ppy/TW and Ppy/TW, confirming the capacitive nature of the Ppy/PVSA thin film material. The capacitive nature may be ascribed to the electrostatic incorporation of anionic dopant into the polypyrrole matrix (Fig. 8). The neutral surfactant composite films did not display this capacitive nature.

3.2.2. Film thickness and mass of polymer deposited

The mass of polymerized material deposited at the Pt working electrodes was calculated from

$$m = \frac{Q_{dep}M}{Fz} \tag{4}$$

where m is the mass of PPY that was deposited on the electrode and Q_{dep} is the deposited charge, M is the molecular weight of pyrrole, F is the Faraday constant and z is the number of electrons involved in the process [16,17].

The thickness of the polymer layer was calculated using,

$$D = \frac{m}{AxL} \tag{5}$$

where D is the density, A is the area of the electrode and m is the mass of the polymer deposited at the electrode and L is the thickness of the layer deposited.

The electrons involved in the process were taken as 2.25 and the density of polypyrrole as 1.5 g cm^{-3} [16] (see Table 1).

The equation used to calculate the surface coverage was,

$$\tau = \frac{Q}{nFA} \tag{6}$$

Q is the deposited charge, τ is the surface coverage.

The product specifications provided by the chemical supplier indicates that TX has the lowest density (1.07 g L^{-1}) compared to PVSA (1.2 g L^{-1}) and TW (1.1 g L^{-1}). The mass deposited and surface coverage follow the trend of product density since the ratio of surfactant to polypyrrole was controlled by equal volume contributions from the surfactant. The trend in density of PVSA, TW and TX, show good agreement with values obtained for mass deposited,

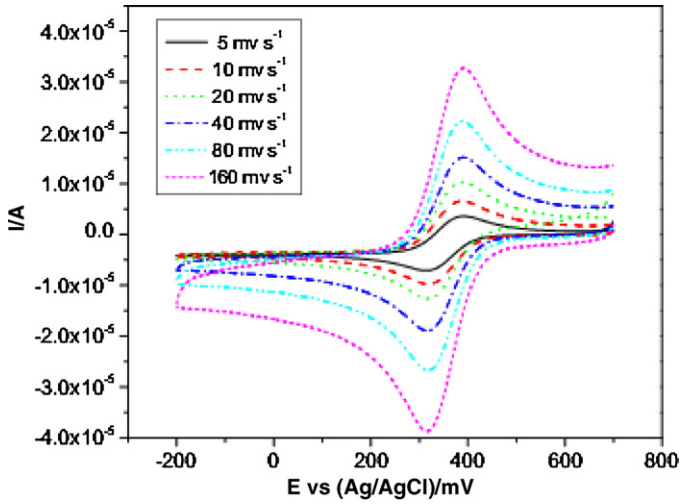

Fig. 6. Cyclic voltammetry of Ppy/TW at Pt electrode in 6 mM $K_3[Fe(CN)_6]$ in 0.1 M HCl at different scan rates.

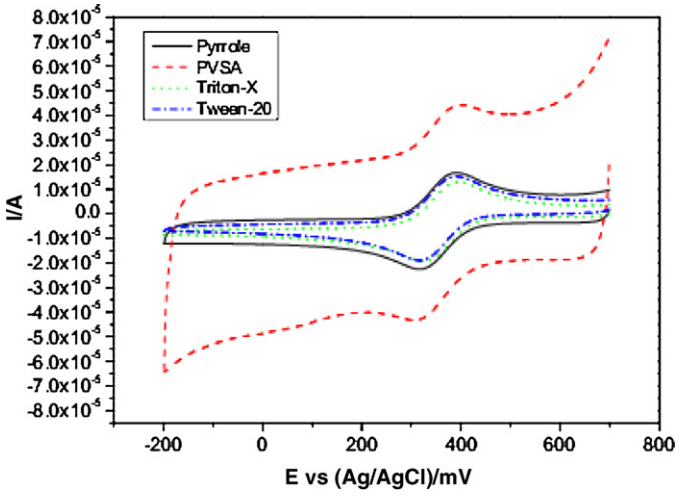

Fig. 8. Polypyrrole and composite materials at 40 mV s^{-1}, in 6 mM $K_3[Fe(CN)_6]$.

Table 1
The surface coverage, mass and thickness of the film of pyrrole and polypyrrole composites in 0.05 M HCl at 15 cycles on Pt against Ag/AgCl (3 M NaCl).

No.	Pt/systems studies	Coverage/mol cm^{-2}	Mass/g	Thickness/cm
1	Pyrrole	3.84E−08	8.82E−08	2.92E−06
2	Pyrrole + PVSA	5.14E−08	1.18E−07	3.91E−06
3	Pyrrole + TX	3.15E−08	7.24E−08	2.40E−06
4	Pyrrole + TW	4.98E−08	1.14E−07	3.79E−06

Table 2
The diffusion coefficients, the heterogeneous rate constants and the peak to peak differences of ferricyanide at the tested electrode assemblies for pyrrole and polypyrrole composites in a 6 mM $K_3[Fe(CN)_6]$ at Pt electrode vs Ag/AgCl (3 M NaCl).

No.	Pt/system	D_R/cm^2 s^{-1}	D_O/cm^2 s^{-1}	k_s/cm s^{-1}	ΔE_p at different scan rate						
					5	10	20	40	50	80	160
1	Pyrrole	8.16E−12	6.73E−12	5.26E−06	84	69	71	73	70	72	80
2	Pyrrole/PVS	8.08E−12	6.29E−12	1.04E−05	66	69	69	77	81	79	91
3	Pyrrole/TX	6.92E−12	5.81E−12	1.4E−06	84	71	66	69	69	69	72
4	Pyrrole/TW	7.3E−12	6.38E−12	1.04E−05	75	68	64	73	73	68	74

surface coverage and film thickness for their respective films (see Table 2).

3.3. Electrochemical impedance spectroscopy

The estimation of kinetic parameters such as diffusion coefficient and charge transfer resistance may also be interpreted from appropriate impedance data. EIS is a widely used versatile technique to characterize organic–inorganic coatings and self-assembled monolayers adsorbed on the surface of an electrode as compared to other techniques [18].

Electro-neutrality within the electro-active conducting polymer film [19] is facilitated by the movement of ions between the polymer and the electrolyte solution and the overall process of oxidation–reduction with doping/undoping of polymer is considered as delocalization of charges and unpaired electrons over a large number of monomer units. Overall, the process includes electron transfer at electrode-film interface, electron and counter ion-transport in the conducting polymer film and diffusion redox-ion transfer (generally linear diffusion) at film–electrolyte interface.

We have modeled our electrochemical cell as two parallel processes characterizing the electron transfer process happening within the conducting polymer film as a result of electron transfer occurring at the film–electrolyte interface due to the redox couple present in the solution. We are using a modified equivalent circuit for the calculation of diffusion coefficient from the impedance data [20] (see Fig. 9)

R_1 represents the resistance to the ionic diffusion of ferricyanide ions into the film, R_{ct} is the charge transfer at the film–electrolyte interface and W_1 represents the Warburg diffusion parameter for the ionic diffusion. Note that the circuit is very similar to an ideal Randle's circuit commonly used to characterize thin films. A distributed impedance element CPE, the constant phase element is introduced because the interface between the film and the electrolyte is not smooth and uniform, comprising of a large number of surface defects as is expected from such surfaces.

A plot of Z' vs $\omega^{-1/2}$ yields a slope of Warburg coefficient σ and intercept equal to $R_s + R_f + R_{ct}$. The Warburg parameter σ and

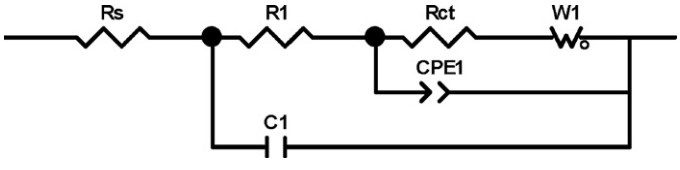

Fig. 9. Circuit diagram used as a fitting model for pyrrole in different surfactants.

diffusion coefficient D can be obtained according to [21]:

$$\sigma = \frac{RT}{n^2F^2A\sqrt{2}}\left(\frac{1}{D_O^{1/2}C_O^*} + \frac{1}{D_R^{1/2}C_R^*}\right) \quad (7)$$

where n is the number of electrons transferred (in this case 1), F is the Faraday's constant (96,485 C mol^{-1}), A is the electrode area (1 cm^2), R is the gas constant (8.314 J mol^{-1} K^{-1}) and T is the room temperature (293 K). Assuming diffusion coefficients $D_{ox} = D_{red} = D$ and concentrations $c_{ox} = c_{red} = C_{bulk}$ we get,

$$D = \left(\frac{\sqrt{2}RT}{n^2F^2A\sigma C_{bulk}}\right)^2 \quad (8)$$

From Eq. (8), the calculated values for diffusion coefficients become approximation values and are called apparent diffusion coefficients.

In order to calculate the rate constants from impedance data, we have used equation,

$$Rct = \frac{RT}{nFi_0} \quad (9)$$

where i_0 is the exchange current in Amperes.

Furthermore,

$$i_0 = nFAk_{et}C_{bulk} \quad (10)$$

Surface coverage can be calculated from [22],

$$\theta = \frac{1 - R_{ct}^{Pt/PPY}}{R_{ct}^{Pt}} \quad (11)$$

and then we can compare this value with the surface coverage calculated from,

$$\tau = \frac{Q}{nFA} \quad (12)$$

After integrating the cyclic voltammetry for polymerization and converting the voltage to time we get the surface coverage as τ.

A plot of Z' vs $\omega^{-1/2}$ is shown below for a 6 mM concentration of $K_3[Fe(CN)_6]$ in 0.1 M HCl at 300 mV potential as chosen from the five potentials recorded, taken the one nearest to the formal potential of the system. The straight line is drawn at the lower frequency side where the Warburg impedance becomes important. For electrochemical systems that are diffusion controlled, the characteristic current phase angle is 45° relative to the frequency. However for complicated systems where the charge transfer constant is finite or chemical kinetic complications occur, the phase angle will differ from 45° and will be a function of excitation frequency [23] (see Fig. 10)

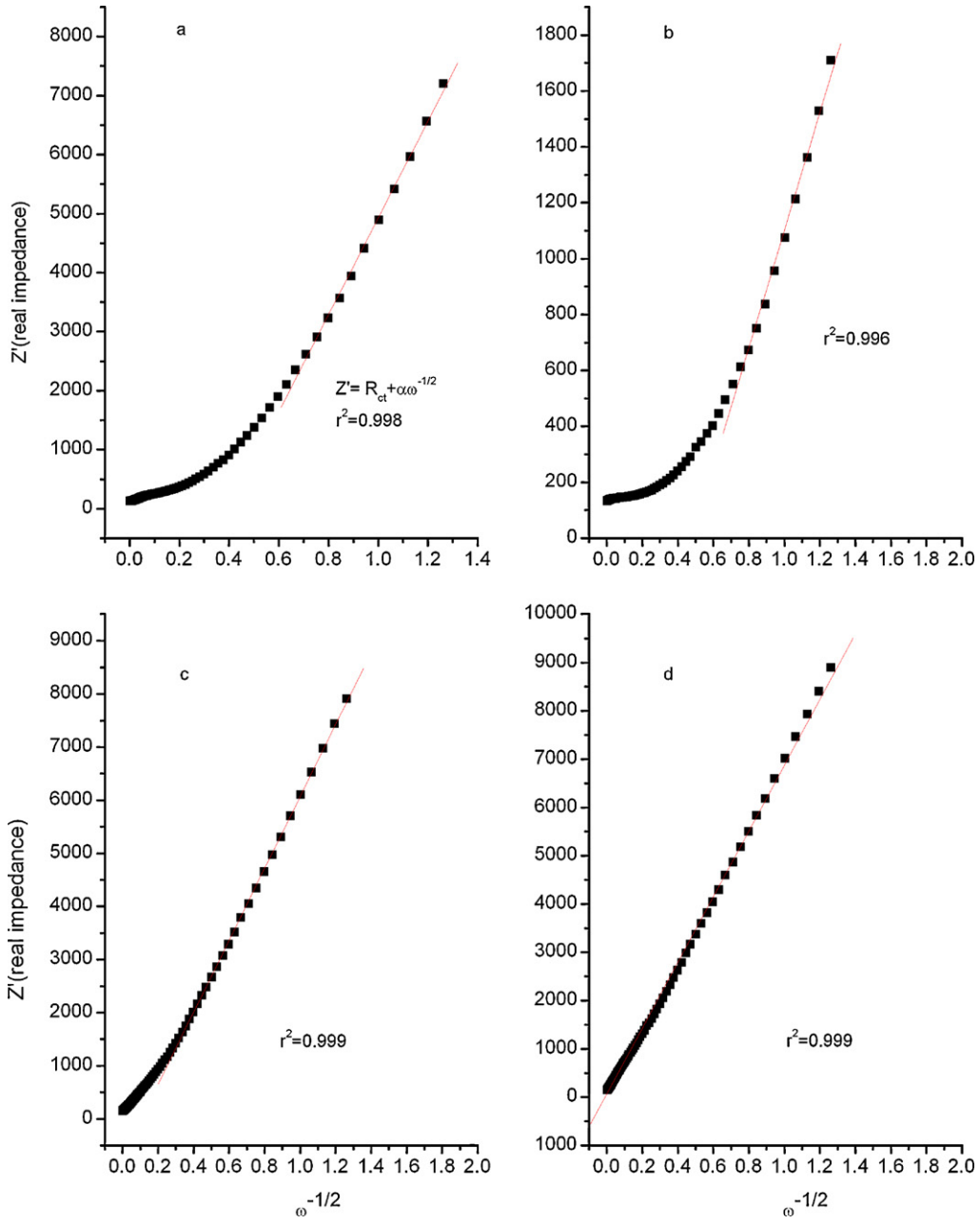

Fig. 10. Plot of Z' vs $\omega^{-1/2}$ at Pt electrode with (a) 0.1 M pyrrole, (b) pyrrole with PVSA, (c) pyrrole with Triton-X 100 and (d) pyrrole with Tween 20, in 6 mM $K_3[Fe(CN)_6]$ and 0.1 M HCl.

Similar data have been plotted for 2 mM and 4 mM $K_3[Fe(CN)_6]$ in 0.1 M HCl at 300 mV in order to compare impedance data within one system and get a relation of diffusion coefficients therein (Fig. 11). The Warburg impedance σ is derived from the slope of Z' vs $\omega^{-1/2}$ and then we calculate apparent diffusion coefficient from Eq. (8)

Furthermore, $i_0 = nFAk_{et}C_{bulk}$

R_{ct} is obtained from the fitting data and inserted into equation below,

$$i_0 = \frac{RT}{nFR_{ct}}$$

and finally k_{et} is calculated,

$$k_{et} = \frac{i_0}{nFAC}$$

Table 3 provides a summary of the computed data.

The determining feature of these composite film electrochemical impedance measurements is the charge transfer resistance and its relation to the Warburg impedance which is controlled by σ. If the system is kinetically sluggish, it will show a large R_{ct} and may display only a very limited frequency region where mass transfer is a significant factor. At the other extreme, R_{ct} might be inconsequentially small by comparison to the ohmic resistance and the Warburg impedance over the nearly whole available range of σ. Then the system is so kinetically facile that mass transfer always plays a role and the semicircle is not well defined [21].

The value of R_{ct} decreases with increasing concentration as it would be expected intuitively implying that the current increases as the concentration increases. Comparison of the computed values showed that PPy/PVSA at 2, 4 and 6 mM is kinetically more

Table 3
The parameters derived from the electrochemical impedance spectroscopy at the Pt electrode for pyrrole and polypyrrole composites doped with different surfactants in 0.1 M HCl.

System	Conc./mmol dm^{-3}	σ/Ω s^{-1}	D/cm^2 s^{-1}	i_0/A	R_{ct}/Ω	k_{et}/cm s^{-1}
Pyrrole	2	8384.89	1.20E−12	6.89E−07	36,585	1.78E−07
	4	6875.51	4.46E−13	9.11E−07	27,676	1.17E−07
	6	7974.68	1.47E−13	8.52E−07	29,586	7.32E−08
Pyrrole+PVSA	2	1755.45	2.74E−11	1.15E−06	22,000	2.95E−07
	4	2165.70	4.50E−12	2.27E−06	11,109	2.92E−07
	6	2093.03	2.14E−12	2.73E−06	9244	2.34E−07
Pyrrole+Triton-X	2	8585.18	1.14E−12	5.95E−07	42,379	1.53E−07
	4	7273.68	3.99E−13	1.18E−06	21,369	1.52E−07
	6	7173.81	1.82E−13	2.68E−06	9427	2.30E−07
Pyrrole+Tween	2	7471.39	1.51E−12	1.89E−06	13,329	4.87E−07
	4	6320.08	5.28E−13	2.13E−06	11,824	2.75E−07
	6	6917.96	1.76E−12	4.95E−06	5097	4.25E−07

Table 4
Comparison of the heterogeneous rate constant as derived from method derived by Nicholson and Shain and from the electrochemical impedance spectroscopy data.

No.	System studied	k_s (Nicholson method)/cm s^{-1}	k_{et} (Imped. Model fitting)/cm s^{-1}
1	Pyrrole	5.26E−06	7.32E−08
2	Pyrrole + PVSA	1.04E−05	2.34E−07
3	Pyrrole + Triton-X	1.4E−06	2.30E−07
4	Pyrrole + Tween	7.72E−06	4.25E−07

facile as compared to other composites. The Warburg impedance σ in relation to the diffusion coefficients were observed to have the lowest values, depicting a kinetically faster system. The values obtained for the rate constant k_{et} supports favoured kinetics at PPy/PVSA interface. Values of diffusion coefficient and rate constant for PPy/TW indicate favorable kinetics at higher frequency, but the overall performance of the system is slowed down by higher Warburg impedance. Theoretical rate constants for the surfactant modified polypyrrole composites (k_s) were calculated by Nicholson and Shain method and compared to rate constants obtained by equivalent circuit modeling (Table 4).

For calculating of k_s, the formula used is from [14] which is,

$$k_s = \frac{\Psi(\pi a D)^{1/2}}{\gamma^{\alpha}}$$

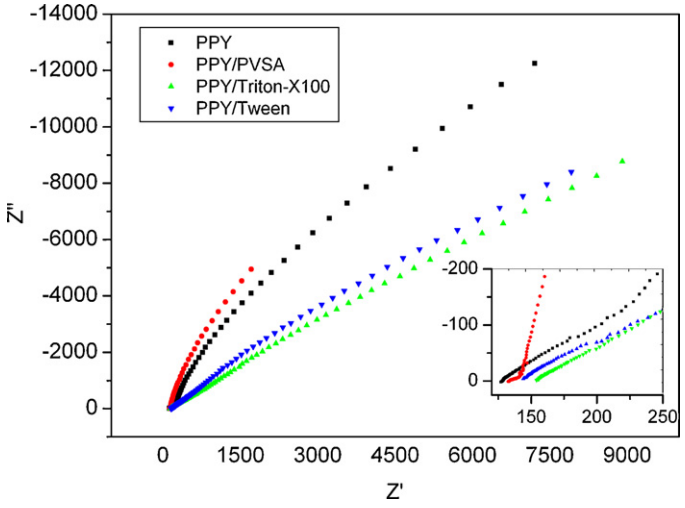

Fig. 11. Electrochemical impedance spectroscopy at the Pt electrode for Ppy, Ppy/PVSA, Ppy/TX and Ppy/TW in 6 mM $K_3Fe(CN)_6$ in 0.1 M HCl.

α is the transfer coefficient taken as 0.5 for simplicity, $\gamma = D_O/D_R$, and $a = nFv/RT$ where v is the scan rate in V s^{-1}. The value for ψ is obtained from the working curves showing dependence of ψ on peak separations. In order to exactly obtain values for the peak separations in different systems, Eq. (3) was used.

We will consider results for 6 mM $[Fe(CN)_6]^{3+}$ in case of rate constants calculated by both method, one is experimentally determined while other is obtained from theoretical considerations.

Rate constant data obtained from equivalent electrical circuit fitting as well as from theoretical considerations indicate that pyrrole/PVSA is indeed the kinetically most facile system. Values of rate constants obtained in this work compare well to the literature values for similar systems. Electropolymerized pyrrole in ET_4NBF_4 at Pt in acetonitrile was shown to have a rate constant value of 1.3×10^{-5} cm s^{-1} [24]. Akinyeye et al., have reported a rate constant of k_s as 2.2×10^{-3} cm s^{-1} for a Pt/Ppy/NQSA in 0.05 M HCl in the absence of any redox probe [25]. Pt/polyaniline in different electrolytes is reported to show k_s in the range of $0.049–5.4 \times 10^{-3}$ cm s^{-1} [26].

4. Conclusion

Anionic and neutral surfactants were observed to have a noteworthy effect on electrochemical kinetics of polypyrrole. Neutral surfactants have little tendency to interact with the hydrophilic homo-polymers and irregular excluded phase separated islands were observed in the surface morphology of the Ppy composites with neutral surfactants. Anionic/cationic surfactants interact broadly with water soluble homo-polymers and produce more homogeneous thin films. The neutral surfactants used in this study do not interact with polypyrrole since it is a hydrophilic homo-polymer and therefore their contribution towards conductivity is not as pronounced as compared to the anionic surfactant. Electropolymerization of polypyrrole in the presence of selective surfactants at a Pt electrode was found to increase the effective surface area of the electrode, which resulted in enhanced interfacial electrochemistry.

Acknowledgement

The authors greatly acknowledge the financial assistance from the department of Chemistry, University of the Western Cape, South Africa.

References

[1] A. Ramanaviciene, A. Ramanavicius, NATO Sci. Ser., II 144 (2004) 287.
[2] S. Sakkopoulos, E. Vitoratos, E. Dalas, Synth. Met. 92 (1998) 63.

[3] J. Barbara, M. Yves, Z. Ze, R. Raynald, S.-L. Marie-Françoise, J.D. Francine, W.K. Martin, D. Lê, L. Gaétan, G. Robert, J. Biomed. Mater. Res. 41 (1998) 519.
[4] Z. Zhang, R. Roy, F.J. Dugre, D. Tessier, L.H. Dao, J. Biomed. Mater. Res. 57 (2001) 63.
[5] W. Zhaoxu, R. Christophe, W. Ying, L.H. Dao, G. Robert, Z. Ze, J. Biomed. Mater. Res. A 66A (2003) 738.
[6] M. Fall, M.M. Dieng, J.J. Aaron, S. Aeiyach, P.C. Lacaze, Synth. Met. 118 (2001) 149.
[7] K. Naoi, Y. Oura, M. Maeda, S. Nakamura, J. Electrochem. Soc. 142 (1995) 417.
[8] Y. Li, S. Zhan, J. Disper. Sci. Technol. 30 (2009) 313.
[9] Y. Li, X. Shi, J. Hao, Carbon 44 (2006) 2664.
[10] M. Omastová, M. Trchová, J. Kovárová, J. Stejskal, Synth. Met. 138 (2003) 447.
[11] Y. Kudoh, K. Akami, Y. Matsuya, Synth. Met. 95 (1998) 191.
[12] Y. Shen, M. Wan, Synth. Met. 96 (1998) 127.
[13] Y. Sun, E. Ruckenstein, Synth. Met. 72 (1995) 261.
[14] R.S. Nicholson, Anal. Chem. 37 (1965) 1351.
[15] I. Lavagnini, R. Antiochia, F. Magno, Electroanalysis 16 (2004) 505.
[16] A.F. Diaz, J.I. Castillo, J.A. Logan, W.Y. Lee, J. Electroanal. Chem. Interf. Electrochem. 129 (1981) 115.
[17] F.-J. Liu, T.-F. Hsu, C.-H. Yang, J. Power Sources 191 (2009) 678.
[18] E. Barsoukov, R. MacDonald, Impedance Spectroscopy: Theory, Experiment and Applications, 2nd ed., John Wiley & Sons, 2005.
[19] C. Deslouis, M.M. Musiani, B. Tribollet, J. Phys. Chem. 100 (1996) 8994.
[20] R.N. Vyas, B. Wang, Int. J. Mol. Sci. 11 (1956).
[21] A.J. Bard, L.R. Faulkner, Electrochemical Methods Fundamentals and Applications, 2nd ed., John Wiley & Sons, Inc., 2001.
[22] O.A. Arotiba, J.H. Owino, P.G. Baker, E.I. Iwuoha, J. Electroanal. Chem. 638 (2010) 287.
[23] P.T. Kissinger, W.R. Heineman, Laboratory Techniques in Electroanalytical Chemistry, 2nd ed., Revised and Expanded, Marcel Dekker Inc., 1996.
[24] J. Tietje-Girault, d.L.C. Ponce, F.C. Walsh, Surf. Coat. Technol. 201 (2007) 6025.
[25] R.O. Akinyeye, I. Michira, M. Sekota, A.A. Al, D. Tito, P.G.L. Baker, C.M.A. Brett, M. Kalaji, E. Iwuoha, Electroanalysis 19 (2007) 303.
[26] R. Pauliukaite, C.M.A. Brett, A.P. Monkman, Electrochim. Acta 50 (2004) 159.